esa

ECOSPHERE

Scale dependence and patch size distribution: clarifying patch patterns in Mediterranean drylands

FERNANDO MELONI,[1,2,]† CRISTIANO ROBERTO FABRI GRANZOTTI,[1] SUSANA BAUTISTA,[2] AND ALEXANDRE SOUTO MARTINEZ[1,3]

[1]*Department of Physics, FFCLRP, University of São Paulo, Ribeirão Preto, SP 14040-901 Brazil*
[2]*Department of Ecology and IMEM, University of Alicante, San Vicente del Raspeig, Alicante 03690 Spain*
[3]*Instituto Nacional de Ciência e Tecnologia em Sistemas Complexos (INCTSC/CNPq), Rio de Janeiro, RJ 22290-180 Brazil*

Citation: Meloni, F., C. R. F. Granzotti, S. Bautista, and A. S. Martinez. 2017. Scale dependence and patch size distribution: clarifying patch patterns in Mediterranean drylands. Ecosphere 8(2):e01690. 10.1002/ecs2.1690

Abstract. In drylands, the underlying vegetation structure is associated with ecosystem functioning and ecosystem resilience. Although scale-dependent patterns are also predicted, empirical evidence often demonstrates that patch sizes are distributed according to a power-law probability distribution function or truncated power-law probability distribution function for a varied range of environmental conditions. Using satellite images and field measures, we assessed the spatial pattern of vegetation patches for a wide range of vegetation cover values in a large set of Mediterranean dryland (MDL) plots, focusing on the statistical distribution function that better fits the patch sizes. We found that power-law or truncated power-law probability distribution function does not always fit the observed patch size frequencies, while lognormal probability density function always fit well to them, implying that the vegetation structure is scale dependent for a large range of conditions. We show how the sampling approach, fit methods, and system dimensionality can affect the patch size distribution, which can explain some conflicting evidence obtained from the empirical data. Our findings question the robustness of criticality as the underlying mechanism driving vegetation patterns in MDLs. The better fit to patch size distribution provided by lognormal as compared with power-law indicates that multiplicative effects of multivariate local influences underlie pattern formation, and suggests that the role of plant–plant facilitation can be overestimated for a large range of conditions.

Key words: complex systems; dryland vegetation dynamics; lognormal distribution; patch size distributions; patch structure; power-law; scale-free systems; self-organized criticality; spatial ecology; spatial patterns.

Received 2 December 2016; accepted 12 December 2016. Corresponding Editor: Debra P. C. Peters.
Copyright: © 2017 Meloni et al. This is an open access article under the terms of the Creative Commons Attribution License, which permits use, distribution and reproduction in any medium, provided the original work is properly cited.
† **E-mail:** fernandomeloni@usp.br

INTRODUCTION

Drylands are regions where the climate is classified as hyper-arid, arid, semiarid, or dry subhumid. Drylands cover approximately 40% of land worldwide, on which more than 2 billion people live (Food and Agriculture Organization of the United Nations 2008). The environmental conditions in drylands are restrictive for many organisms, and the degradation processes in drylands commonly lead to and reflect reduced vegetation, which may cause sudden disruptions to the ecosystem organization (Millennium Ecosystem Assessment 2005). These changes, reported as catastrophic shifts, are related to the loss of resilience and the process of desertification and can be irreversible, with important social, economic, and environmental consequences (Niemeijer et al. 2005, Hammad and Tumeizi 2012, Low 2013). As a result, dryland conservation has gained the attention of governments and social organizations, and many

theoretical and empirical studies have been conducted to reveal the functioning of these ecosystems (Poulsen 2013, Mueller et al. 2014).

The vegetation in drylands forms a mosaic structure in which plant patches are separated by areas of exposed soil (inter-patches). This structure is mainly due to the scarcity of water and nutrients, which limits vegetation growth (Aguiar and Sala 1999, Hochstrasser et al. 2014). Dryland functioning depends on vegetation structure because the size and spatial arrangement of patches can influence water infiltration, nutrient cycling, runoff, and soil stability, as well as the ecosystem response to environmental stress (Puigdefabregas et al. 1999, von Hardenberg et al. 2001, Puigdefábregas 2005, Alados et al. 2006, Bautista et al. 2007, Meron et al. 2007, Thompson 2010, Mayor and Bautista 2012, Mayor et al. 2013, Svejcar et al. 2015). Vegetation patches can also facilitate the establishment of other organisms, thus mediating the resilience and biological diversity of drylands (Bascompte and Rodríguez 2001, HillerRisLambers et al. 2001, Ludwig et al. 2004, Granda et al. 2014). Despite extensive knowledge of the ecological features of drylands, conflicting interpretations of experimental evidence have brought into question some issues regarding vegetation spatial patterns in drylands and the underlying processes that govern the spatial arrangement of patches (Kéfi et al. 2010, 2014, Maestre and Escudero 2010).

The patch size distribution is used to infer the properties of these systems as well as subjacent mechanisms. Empirical data and theoretical models show that vegetation patch sizes in drylands may vary from random to regular (von Hardenberg et al. 2001, 2010, Rietkerk and van de Koppel 2008, Xu et al. 2015*a*), and scale-free patterns are often found (Kéfi et al. 2007, Scanlon et al. 2007, Moreno-de Las Heras et al. 2011, Jeltsch et al. 2014). For instance, Kéfi et al. (2007) assessed drylands from different regions and reported that the non-cumulated patch size distribution in vegetation drylands could be fitted by a power-law probability density function (PL) in well-preserved sites and by a truncated power-law probability density function (TPL) in degraded sites, suggesting that the curve shape could be used as a desertification index. The mechanism proposed for the origin and maintenance of scale-free patterns is a self-organized regime driven by local facilitation and global competition for resources (Kéfi et al. 2007, Scanlon et al. 2007). In this regime, patch size distribution as a PL is expected for two reasons: (1) As a critical phenomenon, it is expected that the geometrical properties of patches show a PL behavior around the critical transition (second-order phase transition; Sahimi 1994) and (2) the aggregation produced by plant–plant facilitation (Kéfi et al. 2007, Xu et al. 2015*a*, *b*) that may result in PL patterns, even when these systems are far from the critical transition.

Because PL behavior is commonly found for several drylands conditions, these systems are, sometimes, interpreted as robust systems (Pascual et al. 2002, Pascual and Guichard 2005, Kéfi et al. 2011, Gowda et al. 2016). In a general sense, the robustness concerns the range of parameter values able to produce a particular pattern: Robustness increases as the range of parameter values increases. Concerning the classical critical systems in percolation problems (Tobochnik 1999, Dakos et al. 2012, van den Berg et al. 2015), a model based on robust critical systems (RCS; Kéfi et al. 2011, Pascual et al. 2002) exhibits less deviation from PL behavior in the neighborhood of the critical point. RCS could explain the widespread scale-free behavior found in empirical data, which is often associated with local facilitation, indicating that a large range of conditions may produce scale-free patterns (Kéfi et al. 2007, Xu et al. 2015*b*). Another regime that can produce frequent PL behaviors is self-organized criticality (SOC). SOC theory explains vegetation patterns found in drylands according to the conditions: a process of recovery and active propagation of disturbance as well the time scale separating both processes. However, as discussed by Scanlon et al. (2007) and Kéfi et al. (2011), the necessary ecological mechanisms to support SOC do not collectively hold for dryland conditions.

Even though several empirical evidences suggest scale-free patterns as ordinary, further evidences point out in another direction. For instance, Maestre and Escudero (2009) assessed a large set of sites from Mediterranean drylands (MDLs) where the frequencies of patch sizes were always fitted by a TPL and never a PL. The authors stated that the shape of the statistical distribution was more correlated with the local soil

properties than with desertification. Furthermore, a model proposed by von Hardenberg et al. (2010) explicitly considered the water resource distribution in soil to explain the emergence of both scale-free and characteristic-length patterns, depending on the parameter setup. von Hardenberg et al.'s model suggests that the speed ratio between spatial distribution of water and water uptake by roots drives the emergence of different patterns because this ratio modulates the range of global competition. In this model, scale-free patterns are only possible in environments in which water diffuses faster than plants can absorb it; when the opposite conditions are present, patterns with a characteristic-length scale are produced. Considering the range of soil properties, terrain conditions, and types of vegetation found in drylands worldwide (Food and Agriculture Organization of the United Nations 2008, 2014, 2015), the findings of von Hardenberg et al. suggest that the conditions able to produce patch sizes distributed as scale-free patterns are unlikely to be an ordinary condition for several drylands. In fact, a recent study (Xu et al. 2015*a*) demonstrated that a characteristic scale can be found in several drylands worldwide. These arguments shed doubts on how frequent the scale-free patterns are in some regions, such as the MDLs of southern Spain, where water remains available for plants for very short periods on the surface and its underground mobility is slow due to soil characteristics (Gallardo 2016).

These empirical evidences concerning patch size distribution have been used to propose a number of models to describe the patch formation in drylands. Such models are able to produce most of the spatial patterns found in empirical data. However, each model approach focuses on a different ecological mechanism or assign different weights to different influences, affecting the global interpretation. It is necessary to take in mind that models can contain many parameters and virtually infinite possibilities of settings, some of them unlikely to occur on field conditions. As stated by Kéfi et al. (2014), theoretical models have been developed faster than field experiments can validate them, and this delay has led to a gap in knowledge of how vegetation patterns are governed in drylands. Not coincidentally, the current conceptual framework concerning vegetation spatial patterns is marked by different points of view, mainly concerning the role of drivers, such as environmental features and biological interactions (Rietkerk et al. 2004, Maestre and Escudero 2009, 2010, Kéfi et al. 2010, von Hardenberg et al. 2010).

Here we call attention for the role of empirical evidences as primary assumptions to formulate conceptual frameworks. For instance, when empirical data are used with these purposes, technical aspects such as sampling techniques and fit methods may lead to misinterpretations. These technical issues may suggest patterns that do not correspond to those really present in nature, resulting in further implications for the interpretation of the ecological system. In the context of dryland vegetation patterns, it is possible that a portion of the conflicting empirical and theoretical evidence might be attributable to problems related to sampling techniques and fit methods.

When heavy-tail distributions are found in empirical data, PL and the lognormal probability distribution function (LNorm) are almost always competing hypotheses, and distinguishing them is not a trivial task (Clauset et al. 2009) and all available tests may not be sufficient to attain a conclusive result (Cirillo 2013). This is a well-known problem in ecology (White et al. 2008) and other areas (Klaus et al. 2011) that are still poorly explored for the patch size distribution in drylands. A deeper implication is that PL or LNorm indicates the involvement of different interaction rules in the problem. Thus, we call attention for the importance to determine the correct path size distribution, because a poor data fit of empirical data or an inadequate sampling technique may lead to a misconception about which forces are governing the patch formation in drylands.

On the one hand, scale-free patterns imply "infinite variance" (even if finite, as in empirical data, it is always very large) and translational invariance. These patterns can emerge from a variety of mechanisms, including critical and non-critical processes (Cross and Hohenberg 1993, Dickman et al. 2000, Bonachela and Muñoz 2009). Interpreting scale-free patterns in dynamic systems (Solé 2011, Dakos et al. 2012), the PL should be associated with the critical phase transition, which is of interest for explaining the catastrophic shifts in drylands. These patterns may also be associated with plant–plant facilitation (Kéfi et al. 2007, Xu et al. 2015*a*, *b*), in a

mechanism that finds analogy in the preferential attachment described for the evolution of scale-free networks (Barabási and Albert 1999). If patch size distribution is a PL, it means that long-range correlations drive the system and that plant–plant interactions (facilitation and competition) are the major influences for the global regime. If PL is a frequent pattern, then RCS and SOC are plausible hypotheses to describe the patch formation.

On the other hand, scale-dependent distributions, such as Gaussian probability distribution function (Normal) and LNorm, are produced by local random effects. For this hypothesis, the underlying mechanism able to explain vegetation patterns are the multiple local environmental influences. Accordingly, the local environmental conditions are determinant for the vegetation growth, producing short-range correlations that result in patch size frequencies distributed as LNorm. This hypothesis implies that the local aspects, such as the cumulated water in the soil, terrain slope, grazing pressure, nutrients, microclimate among other factors, govern the patch growth and are able to produce the general patterns of the system. Systems under these regimes evolve gradually, and the stationary state is determined by a saturation process, which is defined by the local carrying capacity (Vetter 2005). The hypothesis does not exclude the occurrence of PL for some particular set of conditions, but scale-free patterns are restricted to a thin region of the parameter space, generally around critical transitions when they are present (Solé 2011). Systems showing this pattern result in low robustness, meaning that transitions better fit classical percolation problems (Sahimi 1994, Pascual and Guichard 2005). If the patch size distribution shows a characteristic scale for a large range of vegetation covers, the inferred underlying process indicates that short-range correlations are the main drivers of global patterns, whereas further influences, such as plant–plant interactions, are less relevant. Accordingly, the patch size distribution would fit a variety of Normal (additive process) or LNorm (multiplicative process; Mitzenmacher 2003).

In this study, we aimed to investigate the patch size distribution in MDLs from southern Spain (1) using three different data sets of empirical data (from satellite images and field samples), (2) explicitly considering and interpreting the properties and parameters of the statistical distributions that can fit the data, and (3) demonstrating that problems in empirical data fit can lead to misinterpretations about the underlying mechanisms driving the ecological patterns. We used PL, TPL, and LNorm distributions as competing hypotheses, and we determined the best-fit model using different techniques. We also tested whether a scale characteristic can be found in different ranges of vegetation cover, to assess how often scale-free patterns are found or not. We demonstrate that sampling bias may affect the interpretation of the true patterns found in nature, which can lead to misinterpretation of the weight of distinct ecological mechanisms. We conjecture that previously used sampling strategies and data fitting might be responsible for misleading evidence about the distribution of patch sizes in drylands, with consequences for the current theoretical framework.

Methods

Theoretical background

Linking different heavy-tail statistical distributions.—Two of the most important distributions proposed for the frequencies of patch sizes in drylands, the PL and TPL, are specific cases of a very general probability density function (PDF) known as Amoroso (Crooks 2010), also known as generalized gamma PDF (Consul and Jain 1971). The Amoroso also originates an extensive family of further statistical distributions that include the gamma, Normal, and LNorm as well as other distributions commonly reported for biological systems (Crooks 2010). Amoroso is a PDF with four real parameters:

$$f(x) = \frac{1}{\Gamma(\alpha)} \left|\frac{\beta}{\theta}\right| \left(\frac{x-a}{\theta}\right)^{\propto\beta-1} \times \exp\left[-\left(\frac{x-a}{\theta}\right)^{\beta}\right] \quad (1)$$

where a is the location parameter. The scale parameter θ is related to the data of standard deviation. The parameters α and β are the shape parameters and determine the shape of the curve. A noteworthy property of the above PDF is that the metrics used to characterize the shape behavior, such as skewness and kurtosis, only depend on α and β (Granzotti and Souto Martinez 2014). Sampling bias or data treatments that discard extreme values from data have a strong impact on

data dispersion, namely θ. The impact may be greater on the tails of the PDF, which can lead to inaccurate estimates of α and β leading to the identification of different PDFs to represent the same quantity at the same location.

The connections of the parameters α, β, and θ with physical and biological properties are specific to each case. For example, an interesting case for drylands occurs for β = 1 and $a = 0$, resulting in the gamma distribution:

$$f(x) = A \times x^{\alpha-1} \times \exp\left[-\left(\frac{x}{\theta}\right)\right] \quad (2)$$

where $A = 1/\theta^{\alpha}\Gamma(\alpha)$ is the normalization constant. An interesting fact about this particular gamma PDF is that the TPL distribution is represented by the same mathematical expression, $f(x) = Cx^{-\gamma}e^{-(x/x_{\max})}$, although the interpretation of the parameters is slightly different. For TPL, the parameter θ, which is generally interpreted as the dispersion of the distribution, assumes a different interpretation, $x_{\max}$, which is the threshold value of x at which the tail decay is faster than that obtained with the exponent γ of the decaying term $x^{-\gamma}$. When $x_{\max} >> 1$, the exponential term of TPL becomes a constant, and then we have the formula $C \times x^{-\gamma}$, which represents the PL.

Therefore, PL and TPL are obtained from Eq. 1 by fixing their parameters. The last heavy-tail PDF to be considered in our study is the LNorm, which is also a limiting case of the Amoroso. In Eq. 1, we replace α and θ, by writing them as function of β, with $\alpha = 1/\beta\sigma^2$, $\theta = (\beta\sigma)^{2/\beta}$, considering the limit case $\beta \to 0$ (Crooks 2010). The resulting PDF is the LNorm:

$$f(x) = A'' \times x^{-1} \times \exp\left[\frac{1}{\beta\sigma^2}\ln(x) - \frac{1}{\beta^2\sigma^2} \times e^{\beta \ln(x)}\right] \quad (3)$$

or simply

$$f(x) = \frac{1}{x\sigma\sqrt{2\pi}} \times \exp\left[\frac{(\ln(x) - \mu)^2}{2\sigma^2}\right] \quad (4)$$

where μ and σ are the mean and standard deviation, respectively. Considering that a random variable x follows a LNorm, one expects that the transformed variable $Z = \ln(x)$ follows the Normal (Mitzenmacher 2003). It then follows that the logarithmic transformation can be applied to each element of the data set to evaluate whether the transformed data are properly described by the Gaussian distribution.

Fitting empirical data with heavy-tail distributions.—When fitting empirical data, the classical LNorm distribution may be visually distinguished from the PL distribution: By taking the logarithm of the variable, a LNorm has a Gaussian shape, whereas PL data have an exponential shape. These distributions can also be distinguished by plotting data on the log–log scale. The PL distribution in the log–log scale becomes a straight line, whereas the LNorm distribution fits a straight line only in the middle region, and the tail decays faster relative to a PL (or even a TPL) distribution. Errors may appear when data for a random variable that actually follows a LNorm distribution are limited due to sampling or data management biases.

In fact, no purely PL distributions are found in empirical data, and the fit of scale-free distributions is only possible for a limited range of values (Clauset et al. 2009). When fitting PL to empirical data, two non-consecutive steps are required: (1) to find the parameters that better fitted the curve by such exponents, the $x_{\min}$ values (the minimum values in the empirical data that are able to fit a PL), and for TPL, the $x_{\max}$ values (the threshold values at which the decay rate is faster than that with a PL distribution), and (2) discarding alternative hypotheses. Discarding alternative hypotheses is particularly important because statistical distributions such as the LNorm behave as PL functions at a specific range of values, mainly when the exponent of the cumulative probability distribution is approximately 1 (Newman 2005, Guerriero 2012, Cirillo 2013, Deluca and Corral 2013, Virkar and Clauset 2014). Since the hypotheses are conceived a priori, multiple-model comparison can be used to determine the statistical distribution showing the best-fit model. For instance, when the PL is assumed as a feasible pattern to fit the empirical data, the $x_{\min}$ value is calculated, and PL and LNorm are considered as competing hypotheses for the data range limited by $x_{\min}$, but when PL is not a plausible hypothesis, there is no reason to calculate $x_{\min}$.

The solution of this problem is not trivial and is subject of debate in different areas, and care must be taken when interpreting the likely patch

size distribution from empirical data, as we argue below. For instance, Kéfi et al. (2007) and Maestre and Escudero (2009) used recursive 1-d line intercept to sample patches in drylands that were 2-d spatially dispersed and used a binned approach to determine the statistical distribution. The authors found patch sizes distributed as scale-free patterns, which can be actually biased. The 1-d samples can create an important bias in the resulting PDF because large patches (higher diameter) are oversampled, whereas small patches are undersampled, affecting the proportion of distinct patch sizes. Similarly, the construction of bins as regular bins directly from variables or from the log-transformed variable can result in distributions with distinct shapes. When adopting the procedure of log–log plot analysis (White et al. 2008), the empirical data distribution can follow a simple straight line or even an initially straight line followed by moderate decaying of the tail, demanding further tests to determine the real pattern. In turn, these different procedures can produce misinterpretation about the real PDF that describes the frequencies of patch sizes by altering the data dispersion. In these cases, the PL or TPL distributions may be incorrectly considered the best model because the data interval is not suitable to distinguish between LNorm and PL (Boccara 2010). As aforementioned, this type of bias can be of great importance when the underlying mechanisms are thought to reproduce field conditions.

Site description and data acquisition

Our study was conducted in an MDL region in Murcia, southeastern Spain, in the area defined by the coordinates 37°58′6″ N–37°54′25″ N and 1°4′0″ W–0°58′0″ W. The climate is semiarid Mediterranean, with a mean annual rainfall of 297 mm and a mean annual temperature of 19°C (Murcia weather station; 38°0′7″ N–1°10′15″ W; 1984–2010 period). The soils are loamy-silty loam developed over marls and limestones. The landscape in the region is a mosaic of semiarid steppes and open shrublands interspersed with agricultural terraces, most of which are abandoned. The most abundant species in the natural areas are the perennial grasses *Stipa tenacissima* L. and *Brachypodium retusum* (Pers.) P. Beauv., shrubs such as *Anthylis cytisoides* L. and *Rosmarinus officinalis* L., and several chamaephytes, such as *Teucrium polium* L. and *Fumana ericoides* (Cav.) Gand. These steppes and shrublands have been used for grazing, wood gathering, and marginal agriculture for centuries (Puigdefábregas and Mendizabal 1998). At present, most exploitation activities are abandoned, but some marginal grazing still occurs (Verwijmeren et al. 2014).

Using both satellite images (main data source) and field surveys, we assessed the patch size distribution of the natural dryland vegetation in the area at different sampling scales and vegetation cover (V) ranges, which allowed us to also assess whether scale-free patterns are resilient to different field conditions (Bonachela and Muñoz 2009). Concerning the satellite images, we defined 32 square sampling plots of approximately 100 m^2 each (Set_1) and 14 plots of approximately 1000 m^2 each (Set_2) distributed all over the steppe–shrubland slopes in the study area, maximizing the range of vegetation cover values captured by the sampling plots and avoiding areas with clear signs of human interventions, such as paved and unpaved roads, margins of agricultural lands, and watering pools. The 32 plots of Set_1, which was the smallest in size, covered the widest range of vegetation cover (V values between 2% and 96%), totaling 965 patches. For the 14 plots in Set_2, the total number of patches was 4912. The V range was smaller in Set2 (20–64%) than in Set_1, as large areas with large V values are not common in natural semiarid lands. To have a comparable range of V between data sets for the specific analysis of the V effect of patch size distribution, we defined six additional 1000-m^2 plots on areas with exceptionally high cover values that were included in Set_2, resulting in an increased V range (20–79%) for this particular analysis. All color images were acquired from Google Earth (Google 2015), edited, transformed to binary files, and analyzed using the software ImageJ (Schneider et al. 2012, see details in Appendix S1). From these images, we retrieved data on the number and size of patches and on the total vegetation cover in the plot. Patch sizes were measured as the patch area (cm^2) and patch diameters (cm) by geometrical approximation, and these measures were used in different analyses.

The field data (hereafter only as Field) were achieved by field measures. We established 14 sampling plots, of approximately 400 m^2 each.

These field plots were located within the same region that was represented by the images. On each site, we randomly selected five circular parcels of 5 m in radius (~400 m^2 per site), where all patches inside were counted and measured. We measured the diameters, converting to area by geometrical approximation. Therefore, instead of sampling patches using transects by line intercept, 1-d approach, as in Kéfi et al. (2007) and Maestre and Escudero (2009), we sampled the entire area, a 2-d approach, similar to the area used for the images. The vegetation cover in plots ranged between 3% and 85%, totaling 982 patches.

Statistical tests

To determine the statistical distribution that best described the general patch size distribution in each data set, we used all data available (Set_1: data from 32 images; Set_2: data from 14 images; Field: data from 14 sites). Our first test consisted of elucidating how different methods used to create bins can alter the shape of the patch size distribution (Kéfi et al. 2007, 2010, Maestre and Escudero 2009, 2010). As discussed in White et al. (2008), regular bins created directly from raw data tend to underestimate small values with high frequencies by clustering them in only one or few bins. When taking the log-bins, high values with low frequency produce data noise in the tail of the curve. Regular bins created by log-transformed data tend to reduce these two types of bias (White et al. 2008). Then, we apply these two techniques to construct bins: regular bins taken directly from raw data and then their log values, and regular bins taken from the log-transformed data. Thus, we graphically compared these results, making reference to results found by previous authors that assessed empirical data from the same region (Kéfi et al. 2007, Maestre and Escudero 2009, Xu et al. 2015*a*).

Next, we analyzed whether the patch size distribution could fit different heavy-tail PDFs (PL, TPL, and LNorm), which were considered as alternative hypotheses. We also used the Uniform PDF, as a control treatment. We conducted this analysis using two different routines (a set of data analysis and statistical tests). In the first one, we aimed to discard the hypothesis that LNorm could fit patch sizes, and we followed the routine described in Clauset et al. (2009). This routine is described in four steps: (1) $x_{\min}$ values are calculated for the empirical data; (2) only the data range constrained by $x_{\min}$ is used to estimate the parameters of different functions describing distinct statistical distributions (PL, TPL, LNorm, and Uniform); (3) the estimated parameters are used to generate random values showing different distributions (PL, TPL, LNorm, and Uniform), which are considered as alternative hypotheses; and (4) the best-fit distribution is determined by comparison of multiple hypotheses. In the second routine, the PL distribution was not considered a priori as the most important hypothesis to fit the empirical data; that is, the x_{min} value was senseless, and only three of the four steps above described were applied: (2), (3), and (4). The second routine aimed to exclude the scale-free patterns as a plausible hypothesis to fit the empirical data. The main difference between the first and second routines relies on the use of the $x_{\min}$ value and which hypothesis is excluded as feasible. Below, we present the details and implications of each step to clarify this issue.

The first step (1) is to determine $x_{\min}$, the minimal value of x (patch size) in the empirical data that permit fitting of a PL distribution. This step does not guarantee that empirical data are truly distributed as a PL, but it is essential to determine the real exponent γ (the shape of the curve) when data are actually distributed as a PL. The $x_{\min}$ value is acquired by recursive exclusions of minimum values with conjugated data fit using the maximum-likelihood estimation (MLE). Each exclusion of the minimum x-value modifies the γ-value, which leads to a new exclusion of the x-value, until further exclusions do not alter γ further. The process stops when the γ-value stabilizes, yielding the value of $x_{\min}$. Consequently, the $x_{\min}$ determination constrains the empirical data only to the tail part and implies that the first and second routines above differ mainly in the data range. In step 2, the parameter estimation of distinct probability distribution functions (PL, TPL, LNorm, and Uniform) is performed using the goodness of fit, a process that uses conjugated optimization with MLE as method (Clauset et al. 2009). In step 3, the estimated parameters achieved in step 2 are used to generate "expected" values, data vectors, using the inverse of the cumulated distribution functions

(e.g., $y = f(x)^{-1}$). Accordingly, step 3 produces data vectors distributed with the probability functions considered as the alternative hypotheses. In step 4, these "expected" values are considered as competing alternative hypotheses to fit the "observed" values, the vectors containing the empirical data used to estimate the parameters. Next, we calculated the cumulative distribution function (CDF) and the PDF of all "expected" and "observed" raw values, taking regulars bins from log-transformed data. PDF and CDF provide complementary information about probability distributions: Whereas PDF is an intuitive way to analyze data, it is susceptible to fluctuations, while CDF provides better results for data fitting, but low resolution on the tails. A linear regression between each "expected" data vector and the respective "observed" data vector is performed for each probability distribution. Next, we use the Akaike Information Criterion (AIC), with corrections for small samples (AIC_c), to assess the most plausible hypothesis, where the best probability distribution is provided by the goodness of fit (Burnham and Anderson 2002, Mazerolle 2006). We consider as a parameter the ΔAIC_c, where $\Delta AIC_c = AIC - AIC_{min}$, and the best-fit model is given by $\Delta AIC = 0$ (Johnson and Omland 2004). The test also scales the AIC values as weights; probability of each model is the actual best-fit model.

As argued in Xu et al. (2015*a*), plant–plant facilitation is affected by the size of patches. Thus, we do not discharge the hypothesis that patch size distribution could be, even weakly, influenced by vegetation cover. In this sense, we assessed whether the patch size distribution is maintained for different ranges of *V*. For each data set ($Set_1 = 32$ images; enlarged $Set_2 = 20$ images; Field = 14 plots), we created ranges of *V* by clustering the plots in three classes: low cover ($V < 35\%$), medium cover ($35\% < V < 55\%$), and high cover values ($V > 55\%$). Once the best statistical distribution describing patch size frequencies in overall data was found, we used this pattern as reference to analyze patch size frequencies found for different ranges of *V*. Thus, we used the reference distribution to perform CDF plots with upper bounds and lower bounds (10^3 permutation tests; 95% confidence interval), and we calculated the R^2 values to provide the fit quality.

Finally, we assessed whether data sets that actually fit LNorm distributions can fit a PL distribution for specific data ranges. Here, we aim to show how bias from inadequate sampling and/or data handling can possibly lead to misinterpretation about the real statistical distribution. Although patch size is a continuous variable that demands the use of bins (although initially measured as pixels, they are later transformed to area or diameter in units of cm, cm^2, or m^2), we used instead a ranked arrangement of patches for better visualization, from the highest size to the smallest. The procedure consisted of gradually excluding the smallest patches from the analysis, a process similar to the estimation of the x_{min} threshold and the actual exponent value when fitting the PL distributions (White et al. 2008, Clauset et al. 2009). All statistical analyses were performed step by step (no automatic routines), using Microsoft Excel 2013, Statistica 13, and R 2.16 (R Core Team), also using the R package bbmle (Bolker 2016).

Results

Patch size distribution: Is it a scale-free pattern?

In our first test, the statistical distributions of patch sizes (diameters, cm) achieved by different binning methods are compared. As observed in Fig. 1, bins taken from raw data tended to produce a pattern that resembles a "straight" line at the log–log scale, similar to patterns observed by Kéfi et al. (2007) and Maestre and Escudero (2009). This means that data are power-law-distributed, but we point out two additional aspects. First, the higher frequencies (small patches) were all grouped in a few bins, which underestimates the weight of their frequencies and produces bias when assessing the PDF distribution. Furthermore, a few large patches were allocated to several bins, all low frequency, which aggregates data noise in the curve. Hence, when taking bins directly from raw data, an important bias was produced on both sides of the curve, creating an apparent straight line at the log–log scale. As depicted in Fig. 1, this problem was solved by taking bins from the log-transformed variable. The bins constructed from log values provided further details about higher frequencies (small patches) while clustering lower frequencies (large sizes). This approach

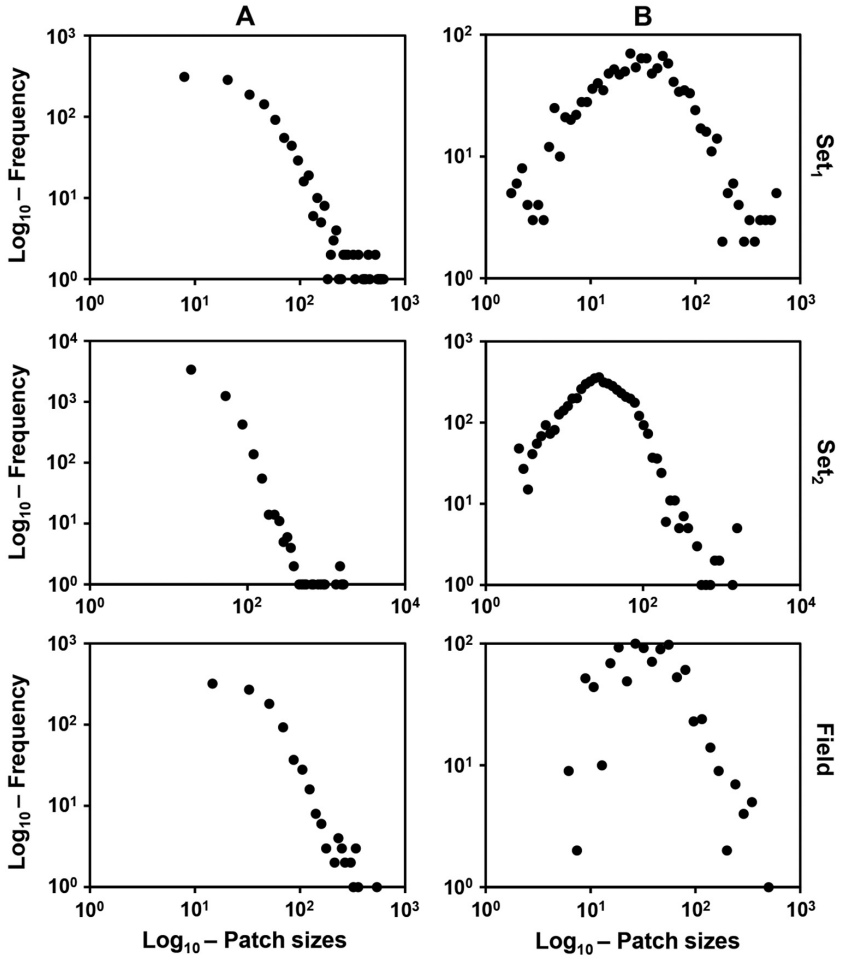

Fig. 1. Different ways to verify patch size distributions in drylands. Set_1: data from 32 satellite images of 100 m^2, n = 965; Set_2: data from 14 satellite images of 900 m^2, n = 4912; Field: data from 14 field samples of ~400 m^2, n = 982. A and B represent different methods to obtain the bins for three different data sets. Patch sizes: diameter (cm). For A, the distribution of patch sizes uses regular bins directly from raw values and results in patterns similar to those found in Kéfi et al. (2007) and Maestre and Escudero (2009). The method used in A shows two well-known problems produced by the method for establishing bins (Clauset et al. 2009, Cirillo 2013). First, a large range of small values is grouped in the same bin, increasing their frequencies in a non-trivial manner. Second, large values show high data noise at the end of the tail. These two effects alter the shape of the distribution, leading to a misinterpretation of the actual statistical distribution of patch size. For instance, the graphics obtained with A indicate that a power-law distribution could fit them well, considering the "apparent" straight line at log–log scale. For B, bins are taken from the Log_{10} of raw values. When this approach is adopted, the puzzling problems common to method A are avoided, providing more confident details about high frequencies and high sizes. When B is adopted, it is clear that the patch sizes are lognormally distributed.

also recovers the patterns observed in Xu et al. (2015*a*). Therefore, when patch size distribution was depicted by the bins obtained from the log-transformed data, a PL distribution was obviously not a plausible hypothesis to fit the entire data range.

Considering all realizations in each data set at a single-log scale (natural logarithm of patch size as area measures, in units of m^2), the histograms obtained for patch sizes indicated that a Gaussian curve was a plausible hypothesis to fit the data distribution (Fig. 2A, D, G). The cumulated

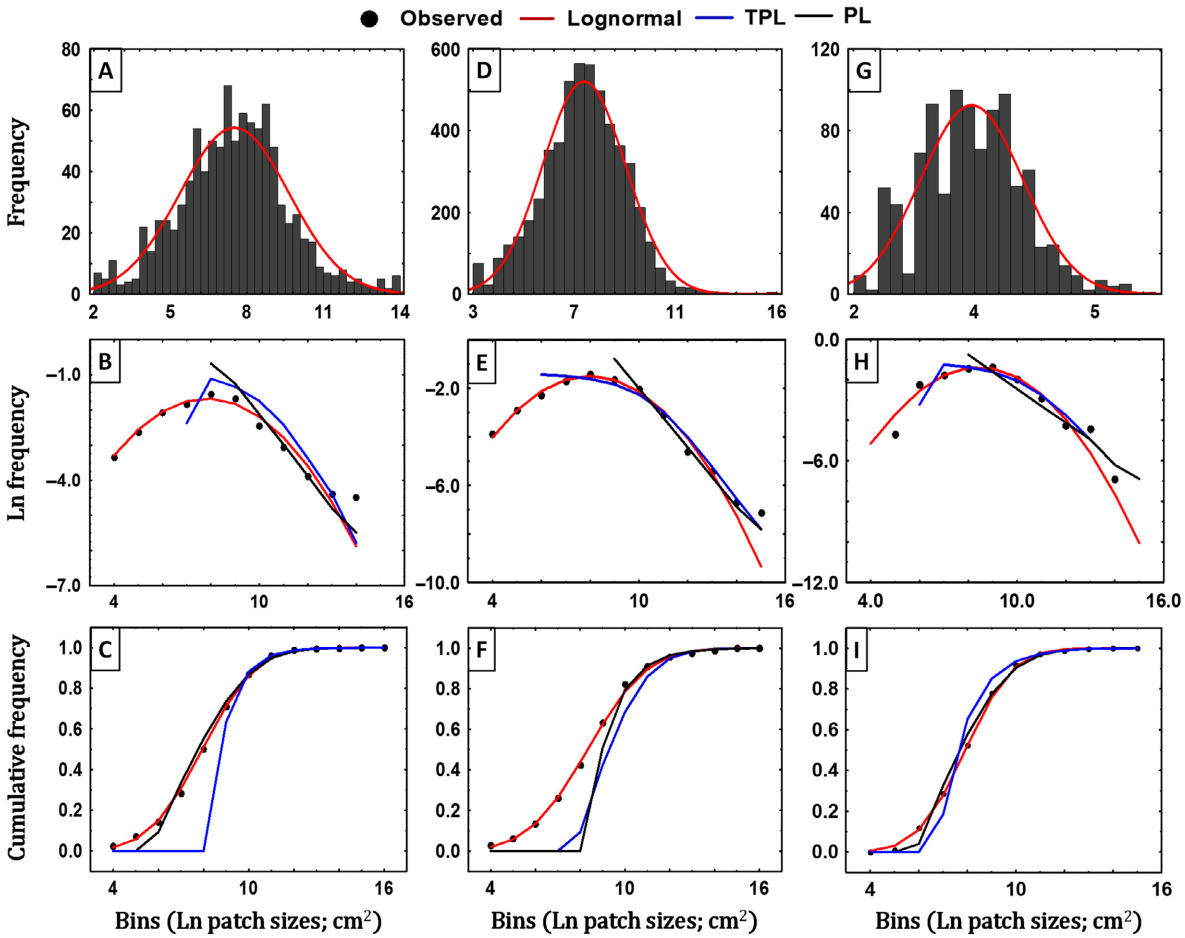

Fig. 2. Frequency of patch size according to different views. A, D, G: histograms, frequencies of patch size according to regular bins created using log-transformed data; B, E, H: PDFs, probability density functions for patch sizes at the log–log scale; C, F, I: CDFs, cumulative density functions for patch size taken at the single-log scale. A–C: data from 32 satellite images (Set_1), n = 965; D–F: data from 14 satellite images (Set_2), n = 4912; G–I: data from 14 field samples, n = 982. The histograms show that when patch sizes are log-transformed (Ln), the frequencies fit well to a Gaussian curve (straight red lines). All images show the entire range of raw data, meaning that x_{min} is not considered. In the PDF cases (B, E, and H), the probabilities are plotted at a log–log scale and show that a lognormal distribution better fits the empirical data than the power-law and truncated power-law distributions, which fit only part of the data range. In the CDF cases (C, F, and I), the cumulative probabilities are plotted at a single-log scale (log-bins), showing the fit quality in a more confident test.

frequencies of patch sizes (single-log) followed a CDF (Fig. 2C, F, I), whereas the log–log scale resulted in a PDF that is fitted as a parabola-like curve (Fig. 2B, E, H). When considering the data range constrained by the x_{min} values, approximately 33% of the data were lost from each data set (both images and field samples), with all patches smaller than 45 cm in diameter discarded. In the case of TPL, the x_{max} values of all data sets suggested that more rapid decays begin for patches approximately 80 cm in diameter, thus indicating that the PL distribution fits well only for values above this threshold.

For data constrained by the x_{min} threshold, the LNorm distribution was the unique plausible distribution fitting the PDF of the empirical data (ΔAIC = 0.0) in all three data sets (Set_1, Set_2, and Field) and the CDF of Set2. For the CDF of Set1 and Field, the LNorm distribution was one of the plausible models able to describe the cumulative

Table 1. Multiple hypothesis test comparisons of different statistical distributions to establish the goodness of fit to patch size distributions in the Mediterranean drylands of southern Spain.

			ΔAIC (Weights)					
			Set_1 image samples		Set_2 image samples		Field samples	
Data range	Function	Par.	CDF	PDF	CDF	PDF	CDF	PDF
Constrained	Uniform	μ	53.1 (0.0)	27.3 (0.0)	110.2 (0.0)	54.4 (0.0)	43.9 (0.0)	31.4 (0.0)
	LNorm	μ; σ^2	0.7* (0.4)	0.0* (1.0)	0.0 (1.0)	0.0 (1.0)	0.6* (0.4)	0.0* (1.0)
	TPL	α; θ	0.0* (0.6)	25.1 (0.0)	40.2 (0.0)	34.4 (0.0)	8.3 (0.1)	11.0 (0.0)
	PL	γ	32.4 (0.0)	15.8 (0.0)	110.2 (0.0)	54.4 (0.0)	0.0* (0.5)	26.9 (0.0)
Unconstrained	Uniform	μ	110.0 (0.0)	54.1 (0.0)	114.8 (0.0)	61.9 (0.0)	85.4 (0.0)	44.9 (0.0)
	LNorm	μ; σ^2	0.0* (1.0)	0.0* (1.0)	0.0* (1.0)	0.0* (1.0)	0.0* (1.0)	0.0* (1.0)
	TPL	α; θ	40.2 (0.0)	34.4 (0.0)	37.5 (0.0)	58.0 (0.0)	26.0 (0.0)	26.9 (0.0)
	PL	γ	60.1 (0.0)	44.9 (0.0)	79.8 (0.0)	61.9 (0.0)	41.3 (0.0)	33.5 (0.0)

Notes: Constrained: fittings that considered only the data range constrained by x_{min}, thus excluding approximately 33% of the data; unconstrained: fittings that considered the full data. *Plausible models ($0.0 < \Delta AIC < 2.0$); weights: relative chance (probability) that the model is the best descriptor. For Set_1 image samples, $n = 965$, $\mu = 7.33$ (log cm^2); $\sigma = 2.16$ (log cm^2); $\alpha = 0.85$; θ-rank = 507; θ-value = 5383 cm^2; $\gamma = 1.14$. For Set_2 image samples, $n = 4912$, $\mu = 7.48$ (log cm^2); $\sigma = 1.75$ (log cm^2); $\alpha = 0.8$; θ-rank = 1500; θ-value = 4417 cm^2; $\gamma = 0.83$. For field samples, n = 982, $\mu = 7.91$ (log cm^2); $\sigma = 2.41$ (log cm^2); $\alpha = 0.8$; θ-rank = 392; θ-value = 4025 cm^2; $\gamma = 1.18$. Par., parameters; CDF, cumulative function distribution; PDF, probability density function; AIC, Akaike Information Criterion.

probabilities (respective ΔAIC values: 0.6 and 0.7; Table 1), with other plausible models including TPL for the Set_1 data (ΔAIC = 0.0) and PL for the Field data (ΔAIC = 0.0). Concerning the unconstrained data (beyond the x_{min} threshold), the best-fit distribution was always achieved by the LNorm distribution for either PDF or CDF (Table 1, Fig. 2). Therefore, the LNorm distribution was a plausible hypothesis to describe the patch size distributions in all cases and was the unique plausible hypothesis for 10 of the 12 combinations of conditions (data range, data set, and type of probability function) assessed.

Considering different sub-samples of several *V* ranges, we found that LNorm distributions always fit the patch size frequencies well, and the adjusted R^2 value for the expected vs. observed values was never below 0.99 (Fig. 3).

Fitting PL and TPL to LNorm-distributed data

Fig. 4 illustrates how disregarding extreme small values in a data set allows us to fit a PL in data that frequencies actually follow a LNorm. The patches from Set_1 (Fig. 4A:E), Set_2 (Fig. 4F:J), and Field (Fig. 4K:O) are ordered from the smallest to the largest size along the *x*-axis. For each data set, the sequence of graphs in Fig. 3 shows the changes in the modal frequencies and the curve shape associated with the gradual exclusion of the smallest patches (i.e., the relative frequencies of large patches are increased). Fig. 4A, F, and K shows the entire data range for each data set. By excluding 30% of patches, patch sizes around the x_{min} values were achieved, and the data also fit well to a TPL (Fig. 4D, I, N). In Fig. 4E, J, and O, the exclusion of the smallest patches reached 50% of the total patches, a threshold near the estimated x_{max} values, and the remaining data can fitted by a PL. For this last case, the ranges of the original data sets are strongly reduced, and by excluding the values with highest noise, that is, 10 to 15 of the largest patches, the remnant data can perfectly be fitted by a PL function (Set_1: $\gamma = 1.1$ and $R^2 = 0.99$; Set_2: $\gamma = 1.1$ and $R^2 = 0.99$; Field: $\gamma = 1.0$ and $R^2 = 0.99$). Thus, data sets that truly follow lognormal distributions may be well fitted by a power-law or truncated power-law distributions at specific data ranges. Notice that exponent $\gamma = 1.1$ is very close to 1.0, which is compatible with that predicted by the lognormal distribution, and is similar to the value previously reported for MDL ($\gamma = 1.2$; Kéfi et al. 2007).

Discussion

Using a multi-scale data set of patch sizes from an MDL region in southeastern Spain, we demonstrated that a LNorm provides a better fit for patch size than PL or TPL. Although scale patterns are reported for patch sizes in some dryland conditions (von Hardenberg et al. 2010,

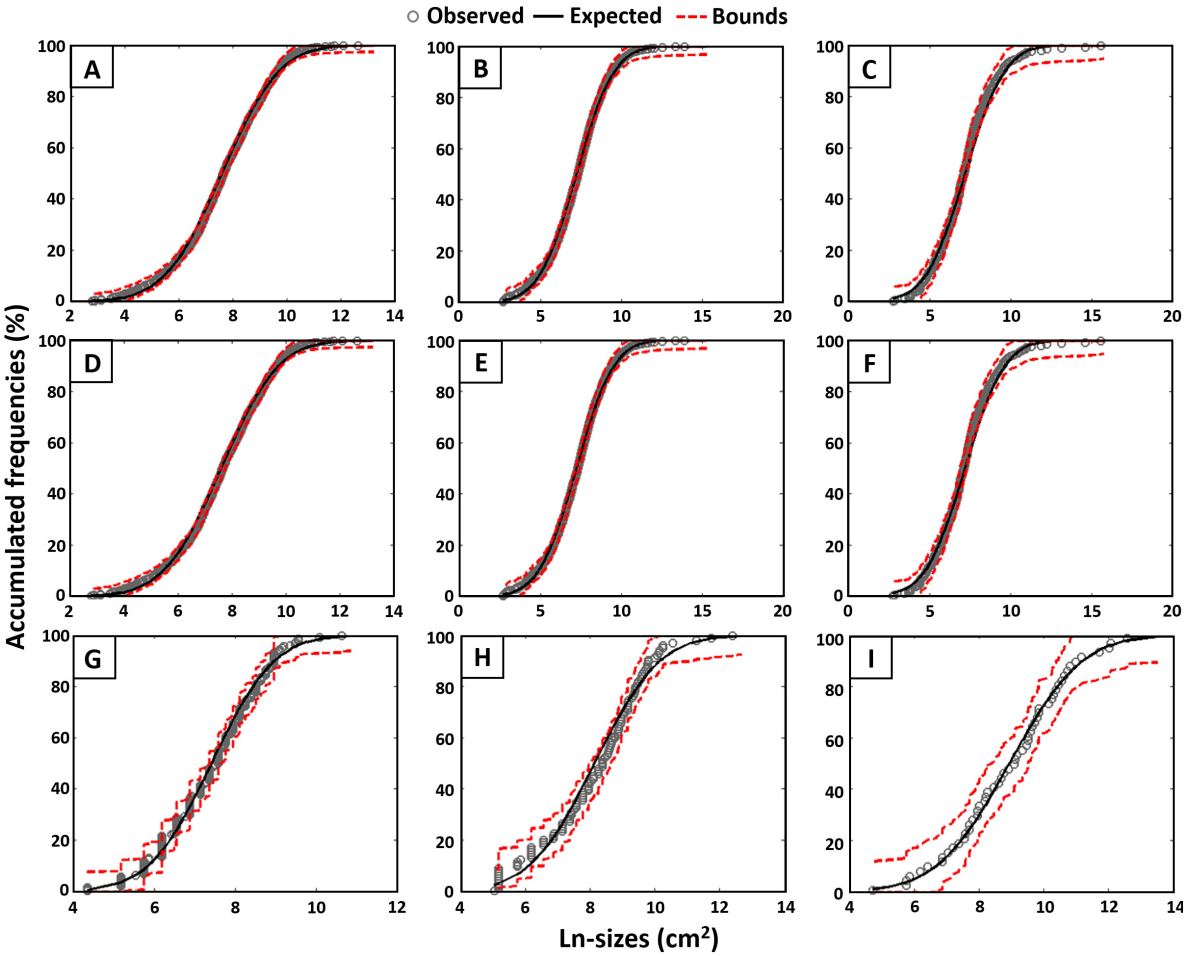

Fig. 3. Fitting the cumulative relative frequencies of patch sizes to a lognormal function for different ranges of vegetation cover (V) found in the Mediterranean drylands. The bins considered the log-transformed area of patches (cm^2), and the adjusted R^2 values were never below 0.98. A, B, C: data from 32 image samples, each representing 10^2 m^2; D, E, F: data from 20 image samples, each representing ~10^3 m^2; G, H, I: data from 14 field samples, each representing ~4 × 10^2 m^2; bounds: confidence interval (95%) for 10^3 permutations.

Xu et al. 2015*a*), our results are not consistent with other results, some of them previously reported for MDLs and for other dryland regions (Kéfi et al. 2007, Scanlon et al. 2007, Maestre and Escudero 2009, Moreno-de Las Heras et al. 2011). The contrasting PDF found in empirical data represents an intriguing problem well known in ecology (White et al. 2008) and other areas (Klaus et al. 2011) that might be explained in terms of the theory of probability functions (Boccara 2010, Crooks 2010). Considering the implications and possibilities produced by data acquisition and treatment on the statistical distributions, we argue that scale-free patterns seem to be not widespread as previously believed.

We demonstrated that sampling and fitting methods can affect the relative frequencies of patch sizes, thus creating technical issues to distinguish among PL, TPL, and LNorm. In fact, sampling and/or binning methods affect the relative weight of small and large patches, as when the smallest patches are gradually eliminated from the analysis (Fig. 4). They may hide the scale of the problem, making PL becomes more plausible (Figs. 1, 4). Hence, PL and TPL may

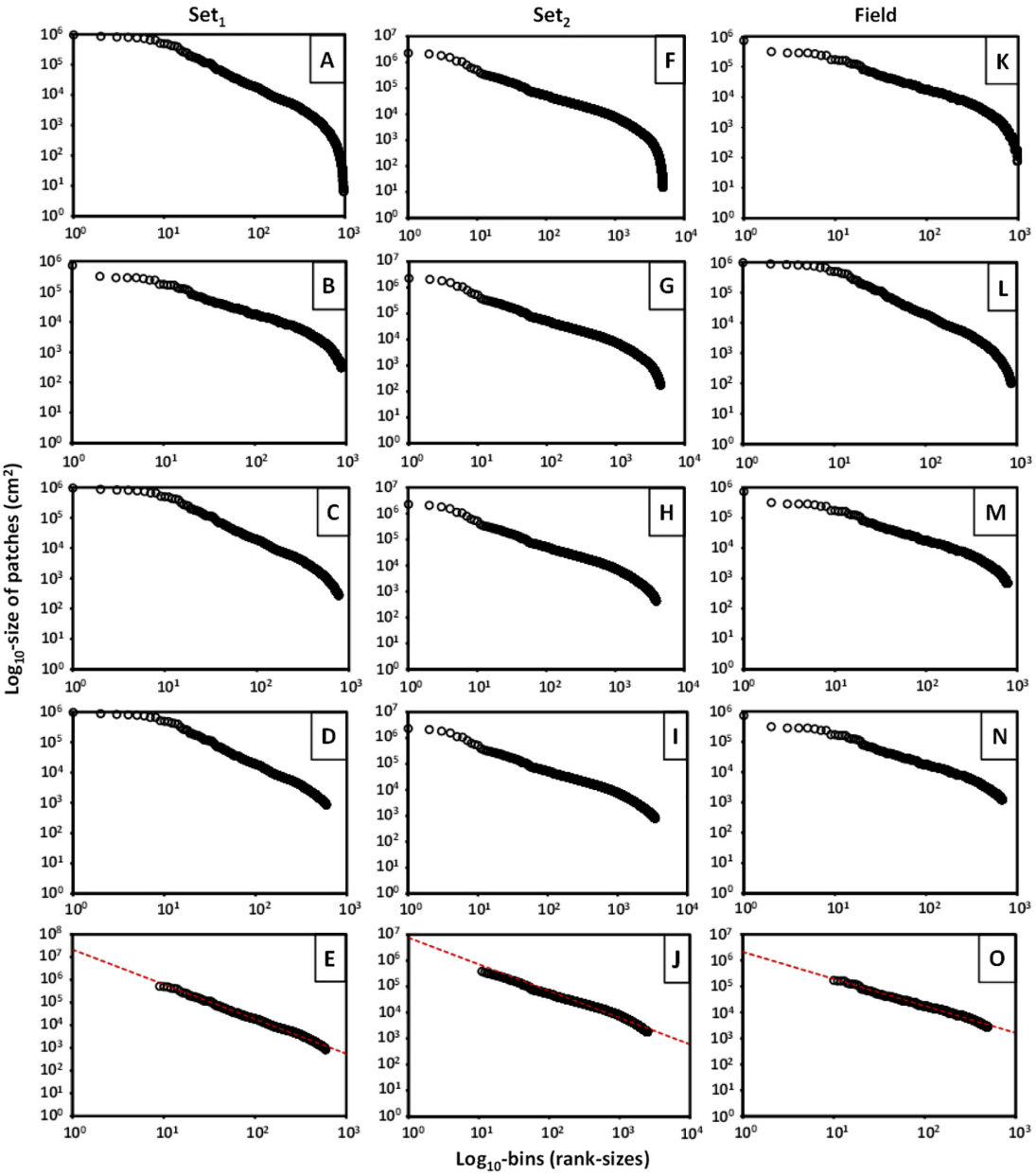

Fig. 4. Effect of sampling that discards small patches when fitting patch size frequencies in the Mediterranean drylands (MDLs). A to E: patches from 32 images (~3200 m^2, $n = 965$); F to J: patches from 14 images (~14,000 m^2, $n = 4912$); K to O: patches from field measures obtained in 14 sites (~5500 m^2, $n = 982$). The truncation process excluded smaller patches, thus changing the shape of the distribution and permitting the conclusion that a power-law distribution is the correct distribution rather than a lognormal distribution. A, F, and K: original curves; B, G, and L: 10% of the smallest patches discarded; C, H, and M: 20% of the smallest patches discarded; D, I, and N: 30% of the smallest patches discarded; E, J, and O: 50% of the smallest patches and some few highest values (higher noise) discarded, thus fitting a power-law function (dashed line). In E, J, and O, the power-law exponents are ≅1, compatible with the exponents found by previous studies in MDLs, and the linear regression (expected vs. observed) is [$R^2 \sim 1$]; if the largest patches are retained, the R^2 value tends to be smaller, and the exponent values tend to be higher.

describe well frequencies in empirical data that actually are distributed according to a LNorm. For instance, Kéfi et al. (2007) and Maestre and Escudero (2009) assessed patch sizes that were sampled using 1-d line intercept and found different types of scale-free patterns (PL and TPL). Although binning method is not explicitly concerned, the sampling by self could produce some type of data bias. Linking the consequences for the distribution shape, changes in the tail decay could lead to misinterpretations of the PL exponents or the type of PDF. Consequently, the underlying dynamics governing the patch pattern might be misinterpreted. As an insight about this issue, although the degradation process tends to change patch size frequencies, the PL exponent fitted to data distributed as LNorm always produces exponent values of approximately 1 for PDF, information that may be used to compare our findings with data from other drylands worldwide.

The evidence reported by Moreno-de Las Heras et al. (2011) regarding patch size distribution as PL bears another important consideration that goes beyond the bins construction and sampling techniques. These authors adopted a much larger scale (km^2) than the scale dealt in this paper. It is well known that the sum of the effects produced by multiple LNorm on different scales can produce true PLs when the variances are very different (Mandelbrot 1983). Accordingly, multiple scales considered together are able to produce emergent patterns, which may be fitted by PL, although the underlying processes concern scales (see Zhao et al. 2015). Unfortunately, very large MDL plots free of the interference of human activity are hard to find and, consequently, to analyze. This was also the case for our study region, limiting further investigation of this subject.

Because PL (or TPL) and LNorm originate from distinct processes, some of which are well known in statistical physics (Mitzenmacher 2003, Boccara 2010), finding the right statistical distribution of empirical data can shed some light on which drives the patch patterns and the physical interpretation of the problem. A PL distribution implies spatial invariance and "infinite" data variance, also indicating that long-range correlations among plants in drylands are the predominant forces in the system. It means that one event affecting a particular plant will be propagated to all other plants. The LNorm distribution implies in scale-dependent patterns, finite variance. It means that only events inside a characteristic scales are correlated and that independent events and local influences are dominant in such case. Since scale invariance is a necessary condition for criticality, our findings do not support any critical transition for the current stage of our target MDL plots. In fact, the evidence concerning LNorm does not exclude the possibility that vegetation can show criticality at some range of parameter space (e.g., at particular vegetation cover), but the lack of evidence associated with scale-free behavior indicates that PL or TPL is not common in the studied region. Therefore, RCS and SOC hypotheses (Roy et al. 2003, Kéfi et al. 2011) are not supported by our data.

A variety of models based on distinct mechanisms have been proposed to explain the self-organization of patch patterns in drylands (Rietkerk et al. 2004, Kéfi et al. 2007, 2011, von Hardenberg et al. 2010). According to the model proposed by von Hardenberg et al. (2010), scale-free patterns are only possible where water diffusivity in soil, or water distribution on surface, is faster than the plant water uptake, while all other conditions produce patterns with a characteristic scale. This change in parameter conditions puts in contrast the limiting factors governing the vegetation growth, from global to local constraints. Our study area shows gentle to steep slopes and silty soils rich in calcium (Gallardo 2016). It means that water runs fast on surface and slow in soil layers, but also means that water is still no long available on surface and may accumulate on soil layers. Although we did not specifically test the ratio between water distribution speed and water uptake, our findings are in accordance with the predictions of the model presented by von Hardenberg and colleagues. The clay-rich soils and the rugged topography found in the studied region should produce short-range correlations and thus patch sizes with a characteristic scale.

Therefore, our hypothesis is that the current framework concerning the role of plant–plant facilitation as driver of vegetation patterns in drylands, possibly, is not applicable for the region evaluated in this paper. In fact, there are further empirical evidences indicating that small patches cannot produce important effects on ecohydrological dynamics (Bautista et al. 2007,

Mayor et al. 2013), which seems to also produce effects on global patch patterns, as the scales found in drylands worldwide (Xu et al. 2015*a*). Our data corroborate these statements and provide a new one. For MDLs from southern Spain, we demonstrate that a characteristic scale of patch sizes is still present for the most common vegetation covers found in the MDL (up to ~60%). It indicates that for the range of conditions assessed in our study, the mechanisms that drive scale-free patterns are not dominant, even though they may be present.

We have not explicitly addressed the intrinsic local factors and control variables in this paper, but the specialized literature provides a variety of examples indicating the existence of these local influences, including water and nutrient availability, terrain slope, climate, and the carrying capacity for vegetation growth (von Hardenberg et al. 2001, Puigdefábregas 2005, Thompson 2010, Barbier et al. 2014, Cerdà et al. 2014). In this sense, we call attention for the aggregate patterns demonstrated in Xu et al. (2015*a*), which are stated as the result of plant–plant facilitation. According to our views about the topic, these patterns could also be explained as "virtual aggregation" (Wiegand and Moloney 2004), the "apparent" aggregation produced by spatial heterogeneity, which is more in accordance with local influences than with plant–plant facilitation. In fact, it is more probable that both local environmental influences and plant–plant interactions affect the patch patterns in drylands, and thus, we highlight the necessity of field studies concerning for which ecological conditions one effect predominates over the other. Our conclusions about scaling and local influences are based on data acquired in a limited region, the MDL, but we argue that Xu et al. (2015*a*) found scales for a wider spectrum of conditions worldwide. Hence, it is possible that our findings might be applicable to further regions, a topic that is still demanding validation.

In summary, our results provide the evidence that the LNorm can be considered a solid model to describe patch size distributions in MDLs to vegetation covers up to 60%. PL and TPL might be explained as statistical artifacts of LNorm, resulting from a variety of technical issues. LNorm emerges from multiple local influences, indicating that terrain conditions are important for producing spatial patterns of vegetation in drylands in a range of conditions. These results question the robustness of criticality in dryland systems and support the role of local environmental influences in shaping dryland vegetation patterns.

Acknowledgments

Thanks to Ramon Vallejo for the comments concerning drylands and Gilberto Medeiros Nakamura for the insights concerning the interpretation of mechanical statistics. Cristiano R.F. Granzotti acknowledges Capes and Alexandre S. Martinez acknowledges CNPq (307948/2014-5) for support. This work was supported by São Paulo Research Foundation (FAPESP) Grant No. 2013/06196-4 and Grant No. 2014/00631-3 and by the projects CASCADE (GA283068), funded by the European Commission, and DRYEX (CGL2014-59074-R), funded by the Spanish Ministry of Economy and Competitiveness.

Literature Cited

Aguiar, M., and O. E. Sala. 1999. Patch structure, dynamics and implications for the functioning of arid ecosystems. Trends in Ecology and Evolution 14:273–277.

Alados, C. L., P. Gotor, P. Ballester, D. Navas, J. Escos, T. Navarro, and B. Cabezudo. 2006. Association between competition and facilitation processes and vegetation spatial patterns in alpha steppes. Biological Journal of the Linnean Society 87: 103–113.

Barabási, A. L., and R. Albert. 1999. Emergence of scaling in random networks. Science 286:509–512.

Barbier, N., J. Bellot, P. Couteron, A. J. Parsons, and E. N. Mueller. 2014. Short-range ecogeomorphic processes in drylands systems. Pages 85–101 *in* E. N. Mueller, J. Wainwright, A. J. Parsons, and L. Turnbull, editors. Patterns of land degradation in drylands: understanding self-organised ecogeomorphic systems. Springer-Verlag, Dordrecht, The Netherlands.

Bascompte, J., and M. Á. Rodríguez. 2001. Habitat patchiness and plant species richness. Ecology Letters 4:417–420.

Bautista, S., Á. G. Mayor, J. Bourakhouadar, and J. Bellot. 2007. Plant spatial pattern predicts hillslope runoff and erosion in a semiarid Mediterranean landscape. Ecosystems 10:987–998.

Boccara, N. 2010. Modeling complex systems. Springer-Verlag, New York, New York, USA.

Bolker, B. 2016. Package "bbmle": tools for general maximum likelihood estimation. https://cran.r-project.org/web/packages/bbmle/

Bonachela, J. A., and M. A. Muñoz. 2009. Self-organization without conservation: True or just apparent scale-invariance? Journal of Statistical Mechanics: Theory and Experiment 2009: P09009.

Burnham, K. P., and D. R. Anderson. 2002. Model selection and multimodel inference: a practical information-theoretic approach. Second edition. Springer-Verlag, New York, New York, USA.

Cerdà, A., F. Gallart, J. Li, V. P. Papanastasis, R. R. Parmenter, L. Turnbull, A. J. Parsons, and J. Wainwright. 2014. Long-range ecogeomorphic processes. Pages 103–109 *in* E. N. Mueller, J. Wainwright, A. J. Parsons, and L. Turnbull, editors. Patterns of land degradation in drylands: understanding self-organised ecogeomorphic systems. Springer-Verlag, Dordrecht, The Netherlands.

Cirillo, P. 2013. Are your data really Pareto distributed? Physica A: Statistical Mechanics and Its Applications 392:5947–5962.

Clauset, A., C. Shalizi, and M. Newman. 2009. Power-law distributions in empirical data. SIAM Review 51:661–703.

Consul, P. C., and G. C. Jain. 1971. On the log-gamma distribution and its properties. Statistische Hefte 12:100–106.

Crooks, G. E. 2010. The Amoroso distribution. arXiv:1005.3274v1 [math.ST]. https://arxiv.org/pdf/1005.3274.pdf

Cross, M. C., and P. C. Hohenberg. 1993. Pattern formation outside of equilibrium. Reviews of Modern Physics 65:851–1112.

Dakos, V., E. H. van Nes, P. D'Odorico, and M. Scheffer. 2012. Robustness of variance and autocorrelation as indicators of critical slowing down. Ecology 93:264–271.

Deluca, A., and Á. Corral. 2013. Fitting and goodness-of-fit test of non-truncated and truncated power-law distributions. Acta Geophysica 61:1351–1394.

Dickman, R., M. A. Muñoz, A. Vespignani, and S. Zapperi. 2000. Paths to self-organized criticality. Brazilian Journal of Physics 30:27–41.

Food and Agriculture Organization of the United Nations. 2008. Water and cereals in drylands. Earthscan Publishing House, London, UK.

Food and Agriculture Organization of the United Nations. 2014. World reference base for soil resources 2014: international soil classification for naming soils and creating legends for soil maps. World Soil Resource Reports 106. Food and Agriculture Organization of the United Nations, Rome, Italy.

Food and Agriculture Organization of the United Nations. 2015. Global guidelines for the restoration of degraded forests and landscapes in drylands: building resilience and benefiting livelihoods. FAO Forestry Paper 175. Food and Agriculture Organization of the United Nations, Rome, Italy. http://www.fao.org/3/a-i5036e.pdf

Gallardo, J. F. 2016. The soils of Spain. Springer, Cham, Switzerland.

Gowda, K., Y. Chen, S. Iams, and M. Silber. 2016. Assessing the robustness of spatial pattern sequences in a dryland vegetation model. Proceedings of the Royal Society A: Mathematical, Physical and Engineering Science 472:1–25.

Granda, E., A. Escudero, and F. Valladares. 2014. More than just drought: complexity of recruitment patterns in Mediterranean forests. Oecologia 176: 997–1007.

Granzotti, C. R. F., and A. Souto Martinez. 2014. Distance statistics in random media. European Physical Journal B 87:87.

Guerriero, V. 2012. Power law distribution: method of multi-scale inferential statistics. Journal of Modern Mathematics Frontier 1:21–28.

Hammad, A. A., and A. Tumeizi. 2012. Land degradation: socioeconomic and environmental causes and consequences in the eastern Mediterranean. Land Degradation and Development 23:216–226.

HillerRisLambers, R., M. Rietkerk, F. van den Bosch, and H. H. T. Prins. 2001. Vegetation pattern formation in semi-arid grazing systems. Ecology 82: 50–61.

Hochstrasser, T., J. D. A. Millington, V. P. Papanastasis, A. J. Parsons, P. P. Roggero, R. E. Brazier, J. Estrany, A. Farina, and A. Puttock. 2014. The study of land degradation in drylands: state of the art. Pages 13–54 *in* E. N. Mueller, J. Wainwright, A. J. Parsons, and L. Turnbull, editors. Patterns of land degradation in drylands: understanding self-organised ecogeomorphic systems. Springer, Dordrecht, The Netherlands.

Jeltsch, F., et al. 2014. Resilience, self-organization, complexity and pattern formation. Pages 55–84 *in* E. N. Mueller, J. Wainwright, A. J. Parsons, and L. Turnbull, editors. Patterns of land degradation in drylands: understanding self-organised ecogeomorphic systems. Springer, Dordrecht, The Netherlands.

Johnson, J. B., and K. S. Omland. 2004. Model selection in ecology and evolution. Trends in Ecology and Evolution 19:101–108.

Kéfi, S., C. L. Alados, R. C. G. Chaves, Y. Pueyo, and M. Rietkerk. 2010. Is the patch size distribution of vegetation a suitable indicator of desertification processes? Comment. Ecology 91:3739–3742.

Kéfi, S., V. Guttal, W. A. Brock, S. R. Carpenter, A. M. Ellison, V. N. Livina, D. A. Seekell, M. Scheffer, E. H. van Nes, and V. Dakos. 2014. Early warning

signals of ecological transitions: methods for spatial patterns. PLoS ONE 9:e92097.

Kéfi, S., M. Rietkerk, C. L. Alados, Y. Pueyo, V. P. Papanastasis, A. ElAich, and P. C. de Ruiter. 2007. Spatial vegetation patterns and imminent desertification in Mediterranean arid ecosystems. Nature 449:213–217.

Kéfi, S., M. Rietkerk, M. Roy, A. Franc, P. C. de Ruiter, and M. Pascual. 2011. Robust scaling in ecosystems and the meltdown of patch size distributions before extinction. Ecology Letters 14:29–35.

Klaus, A., S. Yu, and D. Plenz. 2011. Statistical analyses support power law distributions found in neuronal avalanches. PLoS ONE 6:e19779.

Low, P. S. 2013. Economic and social impacts of desertification, land degradation and drought *in* White Paper I. UNCCD 2nd Scientific Conference, Prepared with the Contributions of an International Groups of Scientists, April 9–12, 2013. UNCCD Secretariat, Bonn, Germany. http://2sc.unccd.int

Ludwig, J. A., D. J. Tongway, G. N. Bastin, and C. D. James. 2004. Monitoring ecological indicators of rangeland functional integrity and their relation to biodiversity at local to regional scales. Austral Ecology 29:108–120.

Maestre, F. T., and A. Escudero. 2009. Is the patch size distribution of vegetation a suitable indicator of desertification processes? Ecology 90:1729–1735.

Maestre, F. T., and A. Escudero. 2010. Is the patch size distribution of vegetation a suitable indicator of desertification processes? Reply. Ecology 91: 3742–3745.

Mandelbrot, B. B. 1983. The fractal geometry of nature. Freeman, New York, New York, USA.

Mayor, Á. G., and S. Bautista. 2012. Multi-scale evaluation of soil functional indicators for the assessment of water and soil retention in Mediterranean semiarid landscapes. Ecological Indicators 20:332–336.

Mayor, Á. G., S. Kéfi, S. Bautista, F. Rodríguez, F. Cartení, and M. Rietkerk. 2013. Feedbacks between vegetation pattern and resource loss dramatically decrease ecosystem resilience and restoration potential in a simple dryland model. Landscape Ecology 28:931–942.

Mazerolle, M. J. 2006. Improving data analysis in herpetology: using Akaike's information criterion (AIC) to assess the strength of biological hypotheses. Amphibia-Reptilia 27:169–180.

Meron, E., H. Yizhaq, and E. Gilad. 2007. Localized structures in dryland vegetation: forms and functions. Chaos 17:037109.

Millennium Ecosystem Assessment. 2005. Ecosystems and human well-being: desertification synthesis. World Resources Institute, Washington, D.C., USA.

Mitzenmacher, M. 2003. A brief history of generative models for power law and lognormal distributions. Internet Mathematics 1:226–251.

Moreno-de Las Heras, M., P. M. Saco, G. R. Willgoose, and D. J. Tongway. 2011. Assessing landscape structure and pattern fragmentation in semiarid ecosystems using patch-size distributions. Ecological Applications 21:2793–2805.

Mueller, E. N., J. Wainwright, A. J. Parsons, and L. Turnbull. 2014. Land degradation in drylands: an ecogeomorphological approach. Pages 1–9 *in* E. N. Mueller, J. Wainwright, A. J. Parsons, and L. Turnbull, editors. Patterns of land degradation in drylands: understanding self-organised ecogeomorphic systems. Springer, Dordrecht, The Netherlands.

Newman, M. E. 2005. Power laws, Pareto distributions and Zipf's law. Contemporary Physics 46:323–351.

Niemeijer, D., J. Puigdefabregas, R. White, R. Lal, M. Winslow, J. Ziedler, S. Prince, E. Archer, and C. King. 2005. Drylands systems. Pages 623–662 *in* U. Safriel and Z. Adeel, editors. Ecosystems and human wellbeing: current state and trends. Island Press, Washington, D.C., USA.

Pascual, M., and F. Guichard. 2005. Criticality and disturbance in spatial ecological systems. Trends in Ecology and Evolution 20:88–95.

Pascual, M., M. Roy, F. Guichard, and G. Flierl. 2002. Cluster size distributions: signatures of self-organization in spatial ecologies. Philosophical Transactions of the Royal Society B: Biological Sciences 357:657–666.

Poulsen, L. 2013. Costs and benefits of policies and practices addressing land degradation and drought in the drylands. Pages 126 *in* White Paper II. UNCCD 2nd Scientific Conference. UNCCD Secretariat, Bonn, Germany. http://2sc.unccd.int

Puigdefábregas, J. 2005. The role of vegetation patterns in structuring runoff and sediment fluxes in drylands. Earth Surface Processes and Landforms 30:133–147.

Puigdefábregas, J., and T. Mendizabal. 1998. Perspectives on desertification: western Mediterranean. Journal of Arid Environments 39:209–224.

Puigdefabregas, J., A. Sole, L. Gutierrez, G. del Barrio, and M. Boer. 1999. Scales and processes of water and sediment redistribution in drylands: results from the Rambla Honda field site in Southeast Spain. Earth-Science Reviews 48:39–70.

Rietkerk, M., S. C. Dekker, P. C. de Ruiter, and J. van de Koppel. 2004. Self-organized patchiness and catastrophic shifts in ecosystems. Science 305:1926.

Rietkerk, M., and J. van de Koppel. 2008. Regular pattern formation in real ecosystems. Trends in Ecology and Evolution 23:169–175.

Roy, M., M. Pascual, and A. Franc. 2003. Broad scaling region in a spatial ecological system. Complexity 8:19–27.

Sahimi, M. 1994. Applications of percolation theory. Taylor and Francis, London, UK.

Scanlon, T. M., K. K. Caylor, S. A. Levin, and I. Rodriguez-Iturbe. 2007. Positive feedbacks promote power-law clustering of Kalahari vegetation. Nature 449:209–212.

Schneider, C. A., W. S. Rasband, and K. W. Eliceiri. 2012. NIH Image to ImageJ: 25 years of image analysis. Nature Methods 9:671–675.

Solé, R. V. 2011. Phase transitions: primers in complex systems. Princeton University Press, Princeton, New Jersey, USA.

Svejcar, L. N., B. T. Bestelmeyer, M. C. Duniway, and D. K. James. 2015. Scale-dependent feedbacks between patch size and plant reproduction in desert grassland. Ecosystems 18:146–153.

Thompson, S. E. 2010. Spatial patterns in dryland vegetation and the significance of dispersal. Thesis. Duke University, Durham, North Carolina, USA.

Tobochnik, J. 1999. Granular collapse as a percolation transition. Physical Review E 60:7137–7142.

van den Berg, J., J. E. Björnberg, and M. Heydenreich. 2015. Sharpness versus robustness of the percolation transition in 2D contact processes. Stochastic Processes and Their Applications 125:513–537.

Verwijmeren, M., M. Rietkerk, S. Bautista, A. G. Mayor, M. J. Wassen, and C. Smit. 2014. Drought and grazing combined: contrasting shifts in plant interactions at species pair and community level. Journal of Arid Environments 111:53–60.

Vetter, S. 2005. Rangelands at equilibrium and non-equilibrium: recent developments in the debate. Journal of Arid Environments 62:321–341.

Virkar, Y., and A. Clauset. 2014. Power-law distributions in binned empirical data. Annals of Applied Statistics 8:89–119.

von Hardenberg, J., A. Y. Kletter, H. Yizhaq, J. Nathan, and E. Meron. 2010. Periodic versus scale-free patterns in dryland vegetation. Proceedings of the Royal Society B: Biological Sciences 277:1771.

von Hardenberg, J., E. Meron, M. Shachak, and Y. Zarmi. 2001. Diversity of vegetation patterns and desertification. Physical Review Letters 87:198101.

White, E. P., B. J. Enquist, and J. L. Green. 2008. On estimating the exponent of power-law frequency distributions. Ecology 89:905–912.

Wiegand, T., and K. A. Moloney. 2004. Rings, circles, and null-models for point pattern analysis in ecology. Oikos 104:209–229.

Xu, C., M. Holmgren, E. H. van Nes, F. T. Maestre, S. Soliveres, M. Berdugo, S. Kefi, P. A. Marquet, S. Abades, and M. Scheffer. 2015*a*. Can we infer plant facilitation from remote sensing? A test across global drylands. Ecological Applications 25:1456–1462.

Xu, C., E. H. van Nes, M. Holmgren, S. Kéfi, and M. Scheffer. 2015*b*. Local facilitation may cause tipping points on a landscape level preceded by early-warning indicators. American Naturalist 186: E81–E90.

Zhao, K., M. Musolesi, P. Hui, W. Rao, and S. Tarkoma. 2015. Explaining the power-law distribution of human mobility through transportation modality decomposition. Scientific Reports 5:9136.

Supporting Information

Additional Supporting Information may be found online at: http://onlinelibrary.wiley.com/doi/10.1002/ecs2.1690/full